

# Exploiting Certified Defences to Attack Randomised Smoothing

Andrew C. Cullen<sup>1</sup> Paul Montague<sup>2</sup> Shijie Liu<sup>1</sup> Sarah M. Erfani<sup>1</sup> Benjamin I.P. Rubinstein<sup>1</sup>

## Abstract

In guaranteeing that no adversarial examples exist within a bounded region, certification mechanisms play an important role in neural network robustness. Concerningly, this work demonstrates that the certification mechanisms themselves introduce a new, heretofore undiscovered attack surface, that can be exploited by attackers to construct smaller adversarial perturbations. While these attacks exist outside the certification region in no way invalidate certifications, minimising a perturbation’s norm significantly increases the level of difficulty associated with attack detection. In comparison to baseline attacks, our new framework yields smaller perturbations more than twice as frequently as any other approach, resulting in an up to 34% reduction in the median perturbation norm. That this approach also requires 90% less computational time than approaches like PGD. That these reductions are possible suggests that exploiting this new attack vector would allow attackers to more frequently construct hard to detect adversarial attacks, by exploiting the very systems designed to defend deployed models.

## 1. Introduction

A well understood property of learned models is that semantically indistinguishable samples can yield different model outputs (Biggio et al., 2013). When constructed deliberately, such samples are known as *adversarial examples*. These examples, and their associated adversarial attacks pose a significant risk for models which are deployed within contexts where incentives to manipulate the output exist. This risk grows all the more when the difference between the example and the original sample point is minimised, as this heightens the difficulty of detecting such examples.

In contrast to detecting examples, *adversarial defences* attempt to mitigate attack effects. While partially successful, these approaches are typically tied to particular attacks, and as such can be evaded by considering different attack pathways. Rather than attempting to defend against specific attacks, *certified guarantees* of adversarial robustness eschew the attacker-defender paradigm by providing a (possibly

high-probability) guarantee that no adversarial examples exist within a bounded region.

It is well known that models endowed with certified guarantees can still admit practical attacks (Cohen et al., 2019). In fact, as we report on, *certified guarantees themselves can be exploited* to more efficiently construct adversarial perturbations. While these perturbations exist outside the certification region, exploiting this previously unavailable attack surface allows for the construction of adversarial perturbations that are smaller than state-of-the-art. Such perturbations have a higher chance to evade detection, even in the case of human-in-the-loop verification systems (Gilmer et al., 2018).

Motivated by the potential for misuse of certifications, we seek to answer the following questions:

1. How should adversarial examples be defined against models defended by Randomised Smoothing?
2. Can current approaches for attacking neural networks be extended to attack certifiably robust models?
3. Is it possible to exploit the nature of certifications to improve the efficacy of constructing adversarial attacks?

The last of these questions is both the most intriguing and concerning, as it suggests that the very tools that we deploy to hinder adversarial attacks may also benefit the attackers.

While uncovering new attacks has the potential to compromise deployed systems, there is a *prima facie* argument that any security provided by ignoring new attack vectors is illusory. Taking such a perspective has allowed security researchers to uncover attack vectors ranging from adversarial examples through to data poisoning, backdoor attacks, model stealing, transfer attacks and more. Within this work we demonstrate how the nature of certified guarantees admits a heretofore undiscovered attack surface, which allows norm-minimising adversarial examples to be detected through what we dub a *Certification Aware Attack*.

## 2. Adversarial Examples

It has been consistently demonstrated that learned models can be exploited to produce highly confident but incorrect

predictions (Szegedy et al., 2013), which can oftentimes be driven by the existence of piecewise-linear intra-model interactions (Goodfellow et al., 2014). While many vectors exist to exploit this vulnerability, within this work we focus exclusively upon mechanisms that construct adversarial perturbations to evaluation-time (rather than training-time) data in a fashion that changes the model’s output class.

The distance between an adversarial example and its corresponding sample point can be a reliable proxy for the *detectability* of the adversarial example (Gilmer et al., 2018) and attacker cost (Huang et al., 2011). While their motivations vary, both attackers and defenders seek to find the distance to the nearest possible adversarial attack

$$r = \arg \min_{\mathbf{x}' \in \Omega} \|\mathbf{x}' - \mathbf{x}\|_p \quad (1)$$

where  $\Omega = \{\mathbf{x}' \in [0, 1]^d \mid F(\mathbf{x}') \neq F(\mathbf{x})\}$

to a sample point  $\mathbf{x} \in [0, 1]^d$  to be attacked. Here  $r$  is the  $p$ -norm distance to the nearest possible adversarial example; and  $F(\mathbf{x})$  is a mechanism that outputs a predicted class.

While many approaches exist for constructing  $\mathbf{x}'$ , within this work we focus upon a set of key, representative techniques, that will serve as the basis of comparison to our new adversarial attack. The first of these is known as the Iterative Fast Gradient Method (Dong et al., 2018) variant of Projected Gradient Descent (PGD) (Carlini & Wagner, 2017), which iteratively constructs adversarial examples by way of

$$\mathbf{x}_{k+1} = P \left( \mathbf{x}_k - \epsilon \left( \frac{\nabla_{\mathbf{x}} J(\theta, \mathbf{x}, y)}{\|\nabla_{\mathbf{x}} J(\theta, \mathbf{x}, y)\|_2} \right) \right) . \quad (2)$$

This process exploits gradients of the loss  $J(\theta, \mathbf{x}, y)$  to construct steps, subject to a step-size weighting parameter  $\epsilon$ , and a projection operator  $P$  that ensures that  $\mathbf{x}_{k+1}$  is restricted to the feasible input space, which is typically  $[0, 1]^d$  for a  $d$ -dimensional input space. Many PGD extensions exist, including momentum-based variants (Dong et al., 2018) and AutoAttack (Croce & Hein, 2020).

Of these extensions, AutoAttack has received significant attention due to its prowess in identifying adversarial examples. In contrast to PGD, which sets a fixed step-size  $\epsilon$ , AutoAttack algorithmically specifies the step-size at each stage of its iterative process in the aide of converging upon adversarial examples with a pre-specified  $L_2$  norm perturbation magnitude (which obtusely is also labelled as  $\epsilon$ ). This pre-specified perturbation is problematic within contexts for which a norm-minimising perturbation is desirable. Our preliminary investigations have suggested that the only way to minimise the perturbation magnitude is to perform a greedy search over a range of possible pre-specified magnitudes, which is inherently problematic due to the computational cost of employing AutoAttack.

Carlini & Wagner (2017) (C-W) construct adversarial perturbations by way of the minimisation problem

$$\min_{\mathbf{x}'} \left\{ \|\mathbf{x}' - \mathbf{x}\|_2^2 + \max \{ \max \{ f_{\theta}(\mathbf{x}')_j : j \neq i \} - f_{\theta}(\mathbf{x}')_i, -\kappa \} \right\} , \quad (3)$$

which constructs an attack  $\mathbf{x}'$  in terms of the trained model  $f_{\theta}(\mathbf{x})$  (with weights  $\theta$ ). Equation 3 then compares the logit value of the target class  $i$  with that of the next most likely class, subject to the parameter  $\kappa$ . The gradients of the solution to this are then solved in the fashion of Equation 2.

The final baseline attack that we will consider is DeepFool, which constructs untargeted  $L_2$ -norm attacks by attacking a linearised variant of the model. This proxy model is then updated using information from the attacks (Moosavi-Dezfooli et al., 2016) in a manner that allows for automatic step-size control.

## 2.1. Certification Mechanisms

Rather than focusing upon any one adversarial example, certification mechanisms conceptually invert Equation 1, using it instead as a framework for attempting to provably guarantee the lack of adversarial examples up to some radius  $r$ . However, attempting such a process directly by rigorously exploring the input space of  $\mathbf{x}'$  to comprehensively define  $\Omega$  would be prohibitively expensive. Instead certification mechanisms typically examine the neighbourhood of  $\mathbf{x}$  to find some proxy to  $r$ , that guarantee (or to high probability ensures) that the predicted class changes.

One common mechanism for constructing such certifications is *randomised smoothing* (Lecuyer et al., 2019), which employs repeated sampling to certify against *additive* perturbations up to some  $L_p$ -norm  $r$  against a *smoothed* version of the classifier, yielding an isotropic region of guaranteed class invariance covering

$$B_P(\mathbf{x}, r) := \{\mathbf{y} \in [0, 1]^d \mid r \geq \|\mathbf{y} - \mathbf{x}\|_P\} . \quad (4)$$

The smoothed classifier involves estimating the expected output of the model under repeated samples of Gaussian noise, such that

$$E_{\mathbf{X}}[\arg \max f_{\theta}(\mathbf{X}) = i] \approx \frac{1}{N} \sum_{j=1}^N \mathbb{1}[\arg \max f_{\theta}(\mathbf{X}) = i]$$

$$\mathbf{X} \stackrel{i.i.d.}{\sim} \mathbf{x} + \mathcal{N}(0, \sigma^2) . \quad (5)$$

Making this approximation makes constructing certifications computationally tractable, but comes at the cost of relaxing the associated guarantees from an absolute absence of adversarial examples to a high probability guarantee.

Numerous mechanisms exist for constructing certifications within such a framework, including differential pri-

vacy (Lecuyer et al., 2019; Dwork et al., 2006), Rényi divergence (Li et al., 2019), and parametrising worst-case behaviours (Cohen et al., 2019; Salman et al., 2019a; Cullen et al., 2022). The latter of these approaches has proved the most performant, and yields certifications that resemble

$$r = \frac{\sigma}{2} \left( \Phi^{-1} \left( \tilde{E}_0[\mathbf{x}] \right) - \Phi^{-1} \left( \hat{E}_1[\mathbf{x}] \right) \right) . \quad (6)$$

In the interests of simplifying notation, we define  $(E_0, E_1) = \text{topk}(E_{\mathbf{X}}[\arg \max_{\theta} f_{\theta}(\mathbf{X}) = i], 2)$  for the two largest class expectations. These quantities are mapped into what are respectively the lower and upper bounds  $(\tilde{E}_0, \hat{E}_1)$  to some confidence level  $\alpha$  (as calculated by way of the Goodman et al. (Goodman, 1965) confidence interval). Beyond this  $\sigma$  represents the level of additive noise, and  $\Phi^{-1}$  is the inverse normal CDF, or Gaussian quantile function.

This is not to say that randomised smoothing is the only mechanism for achieving certifications. Other approaches typically attempt to construct bounding polytopes using either propagating interval bounds through the model (Interval Bound Propagation or IBP); or employing linear relaxation to construct bounding output polytopes over input bounded perturbations (Salman et al., 2019b; Mirman et al., 2018; Weng et al., 2018; Zhang et al., 2018a;b; Singh et al., 2019; Mohapatra et al., 2020), which generally provides tighter bounds than IBP (Lyu et al., 2021).

In contrast to randomised smoothing, IBP and convex relaxation employ augmented training processes to incentivise tight bounds (Xu et al., 2020), which requires significant model re-engineering. Moreover both of these approaches exhibit a time and memory complexity that makes them infeasible for complex model architectures or high-dimensional data (Wang et al., 2021; Chiang et al., 2020; Levine & Feizi, 2020). While the mechanisms that we will describe in the following sections can be applied to these methods, for the remainder of this work we will focus upon the more popular and scalable randomised smoothing.

### 3. Attacking Randomised Smoothing

That randomised smoothing constructs high-concentrated outputs that are nonetheless still random suggests that particular care is required to define what a successful adversarial attack looks like. One approach would be to attack the individual model draws under noise, in a fashion similar to Expectation Over Transformation (Athalye et al., 2018). However, doing so would be inherently inefficient, as the attacker would eschew the advantages gained by the deterministic model structure in certification mechanisms.

Instead we suggest that a successful attack in this context should be one in which an adversarial perturbation  $\delta$  induces

an expected class output change, of the form

$$\begin{aligned} & \arg \max_{i \in \mathcal{K}} E[f_j(\mathbf{X} + \delta) = i] \\ & \neq \arg \max_{i \in \mathcal{K}} E[f(\mathbf{X}) = i] \end{aligned} \quad (7)$$

for some model  $f(\mathbf{x}) \in \mathcal{K}$ . To ensure that this attack is *confident*, and not a product of the uncertainties inherent in the Monte-Carlo expectation process of Equation 5, we add the additional condition that

$$\tilde{\mathbb{E}}_k[f_{\theta}(\mathbf{X} + \delta)] > \hat{\mathbb{E}}_i[f_{\theta}(\mathbf{X} + \delta)] , \text{ for some } k \in \mathcal{K} \setminus i . \quad (8)$$

That the underlying attack framework is still deterministic (with high probability) allows any of the attack frameworks within Section 2 to be applied to this problem space.

The very nature of randomised smoothing would at first principles suggest that it may be easier to attack models employing it as a certification mechanism, as the smoothing process is analogous to a Gaussian blur of the decision space. Such a blurring would likely decrease the local variance of gradients in this space, and make it easier to identify nearby adversarial examples. However, one complicating factor is the presence of nondifferentiable  $\arg \max$  layers at the final layer of models  $f(\mathbf{x})$ . This limitation can be circumvented by any attacker with sufficient access, by replacing  $\arg \max$  layers with the Gumbel Softmax (Jang et al., 2016)

$$y_i = \frac{\exp((\log(\pi_i) + g_i)/\tau)}{\sum_{j \in \mathcal{K}} \exp((\log(\pi_j) + g_j)/\tau)} \text{ for all } i \in \mathcal{K} . \quad (9)$$

The ability of an attacker to modify the final layer to admit differentiation implies that the attacker must have some level of access to the model. However, such a level of access should be considered as a subset—rather than an extension—of the white-box assumption that is implicitly required to access gradient-based information. The only extension to a traditional white-box access model is the need to understand the level of added noise  $\sigma$ .

While such a white-box attack framework is limiting, prior works have demonstrated that it may be possible to successfully attack black-box models by way of surrogate models (Papernot et al., 2017), effectively converting black-box models into white-box models, that are suitable for attack. Moreover, as will be discussed in Appendix C, the attacker does not require exact knowledge of  $\sigma$ , with even approximate values still yielding an attack which exhibits improved performance relative to comparable attacks.

We also emphasise that a number of other approaches can also be employed to circumvent concerns relating to differentiability, including stochastic gradient estimation (Fu, 2006; Chen et al., 2019) and surrogate modelling. However, as the focus of this work is upon the applicability of attacks themselves, we choose to facilitate gradient-based adversarial attacks by way of the Gumbel-Softmax.

#### 4. Certification Aware Attacks

The aforementioned approach allows any attack to be applied to models defended by randomised smoothing. However, we may further improve attack efficiency by exploiting the guarantees of certified robustness to construct smaller adversarial perturbations. This is made possible by considering certifications not as guarantees regarding where adversarial attacks can not exist, but as lower bounds on the space where attacks may exist.

Certifications exist not just at a point of interest, but across the instance space (Cullen et al., 2022). Accordingly, we can exploit not just the sample point’s certification, but at all points along an attack’s iterative sequence. Moreover, once we identify an adversarial example, the certifications associated with successful attacks can be *exploited to minimise the perturbation norm of the attacks themselves*. To achieve this, we begin by solving the surrogate problem

$$\begin{aligned} \hat{\mathbf{x}} = \arg \min_{\hat{\mathbf{x}}} |E_0(\hat{\mathbf{x}}) - E_1(\hat{\mathbf{x}})| \\ \text{s.t. } \arg \max f(\hat{\mathbf{x}}) = f(\mathbf{x}) \end{aligned} \quad (10)$$

This formalism may seem counter-intuitive: the constraint ensures that  $\hat{\mathbf{x}}$  cannot be an adversarial example. However, consider the gradient-based solution of the previous problem

$$\mathbf{x}_{i+1} = P \left( \mathbf{x}_i - \epsilon_i \left( \frac{\nabla_{\mathbf{x}_i} |E_0[\mathbf{x}_i] - E_1[\mathbf{x}_i]|}{\|\nabla_{\mathbf{x}_i} |E_0[\mathbf{x}_i] - E_1[\mathbf{x}_i]|\|} \right) \right) \quad (11)$$

for which each  $\mathbf{x}_i$  has associated certifications  $r_i$ . If we were to set that  $\epsilon_i \leq r_i$ , then by Equation 10 we can confidently state that  $\mathbf{x}_{i+1}$  will always predict the same class as  $\mathbf{x}_i \forall i \in \mathbb{N}$ , as each new sample does not move beyond the certified radius of the prior point, and thus  $\mathbf{x}_{i+1}$  cannot elicit a change in the output class. However if we instead impose that  $\epsilon_i \geq r_i$ , we ensure that the new candidate solution  $\mathbf{x}_{i+1}$  outside the region of certification of the previous point. Doing so is a *necessary but not sufficient* condition for identifying an adversarial example.

##### 4.1. Specifying $\epsilon_i$

One mechanism for ensuring that  $\epsilon_i \geq r_i$  would simply be to set the  $\epsilon_i$  of Equation 11 to be

$$\epsilon_i = r(\mathbf{x}_i) (1 + \delta) \quad , \quad (12)$$

for some  $\delta > 0$ . However, in doing so we are only taking into account the region of certification at  $\mathbf{x}_i$ , rather than for all  $\mathbf{x}_j$  for  $j = 0, \dots, i$ . The additional information about the potential region within which adversarial examples exist

can be factored in by instead defining

$$\begin{aligned} \epsilon_i &= (1 + \delta) \arg \max_{\hat{\epsilon}} \|\hat{\mathbf{x}}(\hat{\epsilon}) - \mathbf{x}_i\| \\ \text{s.t. } \hat{\mathbf{x}}(\hat{\epsilon}) &\in \bigcup_{j=0}^i B_P(\mathbf{x}_j, \mathbb{1}_{c_0=c_j} r_j) \quad \forall \tilde{\epsilon} \in [0, \hat{\epsilon}], \\ \text{where } c_i &= \arg \max_{i \in \mathcal{K}} E[f(\mathbf{x}) = i] \\ \text{and } \mathbb{1}_{c_0=c_i} &= \begin{cases} 1 & \text{if } c_0 = c_i \\ 0 & \text{if } c_0 \neq c_i \end{cases} \end{aligned} \quad (13)$$

for an  $\mathbf{x}_{i+1}(\epsilon_i)$  as defined by Equation 11.

This condition attempts to find the step size  $\epsilon_i$  that maximises the distance between  $\mathbf{x}_i$  and a new candidate solution  $\hat{\mathbf{x}}$ , while ensuring that the vector spanning  $\mathbf{x}_i$  and  $\hat{\mathbf{x}}$  remains strictly inside the region of previously certified examples predicting the same class as the original sample point  $\mathbf{x}_0$ .

The multiplicative factor of  $(1 + \delta)$  ensures that the new candidate solution remains outside the region of prior certification if  $\delta > 0$ . However, in practice taking such large steps may be disadvantageous in certain contexts, and as such in practice we define  $\epsilon_i$  such that

$$\tilde{\epsilon}_i = \text{clip}(\epsilon_i, \epsilon_{\min}, \epsilon_{\max}) \quad , \quad (14)$$

where  $\tilde{\epsilon}_i$  and  $\hat{\epsilon}_i$  are pre-defined lower- and upper-bounds upon  $\epsilon_i$ . The details of how these parameters can be set experimentally can be found in Appendix B.

##### 4.2. Refining Adversarial Examples

The logic behind exploiting certifications to help guide identifying adversarial examples can also be applied to *refine* any identified examples. In doing so, we are able to minimise the perturbation norm, and ideally decrease the detectability of the attack. To achieve this, consider the point  $\mathbf{x}_i$ , which results in a class prediction  $c_i \neq c_0$  and certification radii  $r_i$ . The very nature of this certification guarantees that a step of size  $\epsilon_i \leq r_i$  will produce a class prediction  $c_{i+1} = c_i \neq c_0$ , leading to the iterative scheme

$$\mathbf{x}_{i+1}(\epsilon) = \mathbf{x}_i + \epsilon \frac{\mathbf{x}_0 - \mathbf{x}_i}{\|\mathbf{x}_0 - \mathbf{x}_i\|} \quad (15)$$

$$\text{where } \epsilon_i = (1 - \delta) \arg \min_{\hat{\epsilon}} \|\hat{\mathbf{x}}(\hat{\epsilon}) - \mathbf{x}_0\|$$

$$\text{s.t. } \mathbf{x}_i + \tilde{\epsilon} \frac{\mathbf{x}_0 - \mathbf{x}_i}{\|\mathbf{x}_0 - \mathbf{x}_i\|} \in \bigcup_{j=0}^i B_P(\mathbf{x}_j, \mathbb{1}_{c_0 \neq c_j} r_j) \quad \forall \tilde{\epsilon} \in [0, \hat{\epsilon}]$$

At first glance, this may appear to be a restatement of Equation 13 subject to a modified condition on the set of  $B_P$ , however there are key differences in both the equations themselves and their implications. While Equation 13 attempts to identify the largest adversarial step size that ensures that



$\mathbf{x}_{i+1}$  moves outside the region certified by all previous elements in the sequence, Equation 15 instead identifies the largest step size perturbation that minimises the norm distance to  $\mathbf{x}_0$  while retaining an adversarial perturbation relative to this points predicted class.

It must be emphasised though that this framing ensures that  $c_i = c_j \forall j > i$ —that is, once an adversarial example predicting a particular class has been identified, any subsequent adversarial examples will share the same prediction class. As such, even if the model is able to find the smallest adversarial example for the predicted class reached by this sequence, if the model is not a binary classifier it may be that there exists some adversarial example  $\mathbf{x}''$  such that

$$\|\mathbf{x}'' - \mathbf{x}_0\| < \|\mathbf{x}_i - \mathbf{x}_0\| \quad \forall i \in \mathbb{N}.$$

While the above may be true, we emphasise that this process still has the potential to yield significantly smaller adversarial perturbations than can be identified through other techniques, a result that is made possible by exploiting the additional attack surface introduced by certified robustness.

### 4.3. Algorithm

The aforementioned processes can be distilled into Algorithms 1, 2 and 3, the latter of which can be found within Appendix A. Algorithm 1 summarises the process of identifying a norm-minimising adversarial example  $\mathbf{x}'$ , that induces a change in class prediction from  $\mathbf{x}$ . To ensure that a confident adversarial attack—in which  $\hat{E}_0 > \hat{E}_1$ —is achieved the iterative process begins with Line 17 minimising the gap between  $\hat{E}_0$  and  $\hat{E}_1$ , with each iterative step constructed such that the candidate attack is taken outside the certified radii of each prior sample.

Once a sample is found that changes the predicted class, but does not yet yield a confident solution, Line 13 then attempts to maximise  $\hat{E}_0 - \hat{E}_1$ . Once a confident solution has been found Line 7 minimises the norm difference between  $\mathbf{x}'$  and  $\mathbf{x}$ . This step, while ostensibly trivial, is given utility by the constraint of Line 11, which ensures that the candidate solution remains within region of samples which predict the adversarial class. A high level summary of this process can be seen within Figure 1. Starting from an initial sample point of interest, we construct a  $B_P(\mathbf{x}, r)$  describing the region of guaranteed class invariance for our learned function  $f(\mathbf{x})$ .

## 5. Results

To assess our newly identified attack vector, we focus our experiments in two primary directions: against the representative approaches outlined within Section 2; and against the certified guarantees provided by Equation 6. The first of these comparisons is intended to demonstrate progression over state of the art, while the second is intended to eluci-

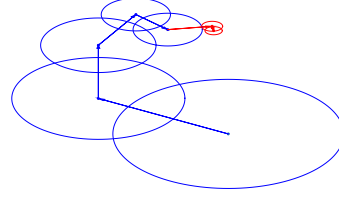


Figure 1. Diagrammatic Representation of the process outlined within Algorithm 1. Here blue and red circles respectively represent certifications of the label class and certifications of an adversarial class, with arrows representing steps of the iterative process.

Table 1. Metrics for MNIST (M), CIFAR-10 (C), and Imagenet (I) across  $\sigma$ , covering the proportion of successful attacks, and the proportion of attacks which outperform all other approaches (*Succ.* and *Best*); the median attack size and time ( $r_{50}$  and *Time* (s)); and the percentage difference to the certified guarantee of Cohen et al.

Data	Type	Smallest Attack				
		Succ.	Best	$r_{50}$	%-C	Time
M-.5	Ours	65%	51%	1.86	56	0.46
	PGD	51%	15%	1.81	54	2.50
	C-W	93%	17%	8.67	605	1.37
	Auto	81%	17%	5.50	357	47.2
	Fool	4%	0%	8.42	2126	0.16
M-1	Ours	100%	97%	2.46	58	0.45
	PGD	68%	2%	2.19	68	2.41
	C-W	94%	0%	9.50	494	1.06
	Auto	100%	0%	6.80	338	45.5
	Fool	43%	0%	16.53	1503	0.15
C-.5	Ours	91%	83%	0.91	56	0.22
	PGD	88%	7%	0.96	65	2.65
	C-W	91%	1%	6.74	865	1.35
	Auto	99%	9%	4.00	495	49.6
	Fool	85%	0%	2.94	486	0.16
C-1	Ours	100%	94%	1.32	67	0.30
	PGD	94%	4%	1.45	90	2.60
	C-W	96%	0%	7.19	751	1.16
	Auto	96%	1%	4.99	493	48.9
	Fool	98%	0%	3.32	457	0.17
I-.5	Ours	54%	71%	1.03	123	3.12
	PGD	59%	13%	1.25	141	31.0
	C-W	56%	16%	33.56	4248	28.2
	Fool	54%	0%	3.08	663	4.59
I-1	Ours	40%	48%	1.10	227	4.08
	PGD	46%	12%	1.68	254	31.0
	C-W	70%	20%	36.10	2998	24.4
	Fool	67%	20%	5.88	748	4.61

**Algorithm 1** Certification Aware Attack Algorithm.

---

```

1: Input: data  $\mathbf{x}$ , level of additive noise  $\sigma$ , samples  $N$ ,
   iterations  $M$ , true-label  $i$ , minimum and maximum step
   size  $(\epsilon_{\min}, \epsilon_{\max})$ , scaling factors  $(\delta_1, \delta_2)$  [where  $\delta_1 \in$ 
    $(0, 1)$  and  $\delta_2 \in (1, \infty)$ ]
2:  $\mathbf{x}', \mathbf{x}'_s, m = \mathbf{x}, \mathbf{0}, \infty$ 
3:  $\mathcal{S}_i = \emptyset \forall i \in \mathcal{K}$ 
4: for 1 to  $M$  do
5:    $\mathbf{y}, \tilde{E}_0, \hat{E}_1, r = \text{Model}(\mathbf{x}'; \sigma, N)$  {Detailed in Algo-
     rithm 2}
6:   Append  $(\mathbf{x}', r)$  to  $\mathcal{S}_{\arg \max \mathbf{y} = i}$ 
7:   if  $\arg \max_{j \in \mathcal{K}} y_j \neq i$  then
8:     if  $\tilde{E}_0 > \hat{E}_1$  then
9:        $d = \nabla_{\mathbf{x}'} (\|\mathbf{x}' - \mathbf{x}\|)$ 
10:      if  $\|\mathbf{x}' - \mathbf{x}\| < m$  then
11:         $m, \mathbf{x}'_s = \|\mathbf{x}' - \mathbf{x}\|, \mathbf{x}'$  {New smallest pertur-
          bation has been identified}
12:      end if
13:       $\epsilon = \text{Algorithm 3}(\mathcal{S}_{\arg \max \mathbf{y} \neq i}, \mathbf{x}', d, r)$ 
14:       $\epsilon = \text{clip}(\delta_1 \epsilon, \epsilon_{\min}, \epsilon_{\max})$ 
15:    else
16:       $d = -\nabla_{\mathbf{x}'} (\tilde{E}_0 - \hat{E}_1)$ 
17:       $\epsilon = \epsilon_{\min}$  {When  $\tilde{E}_0 < \hat{E}_1$  it must be that  $r = 0$ .
        Setting  $\epsilon = \epsilon_{\min}$  avoids this}
18:    end if
19:     $\mathbf{x}' = P(\mathbf{x}' - \epsilon \frac{d}{\|d\|_2})$  {Project upon  $[0, 1]^d$ }
20:    else if  $\arg \max \mathbf{y} = i$  then
21:       $\epsilon = \text{Algorithm 3}(\mathcal{S}_{\arg \max \mathbf{y} = i}, \mathbf{x}', d)$ 
22:       $\epsilon = \text{clip}(\delta_2 \epsilon, \epsilon_{\min}, \epsilon_{\max})$ 
23:       $\mathbf{x}' = P(\mathbf{x}' + \epsilon \frac{\mathbf{x}_0 - \mathbf{x}'}{\|\mathbf{x}_0 - \mathbf{x}'\|})$ 
24:    end if
25:  end for
26: return  $m, \mathbf{x}'_s$ 

```

---

date the difference between the size of certified guarantees—which are a *conservative bound* upon the size of adversarial perturbations—against realisable adversarial attacks. The gap between the best performant attacks and the certified guarantees in turn can be considered as evidence for the potential to improve either certifications, attacks, or both.

To aide in these comparisons, we introduce the concept of the *attack proportion*: the proportion of correctly predicted samples that have an identified attack below a given  $L_2$ -norm radius. As the certified radius provides a lower bound on the size of any individual attack, the largest attack proportion at any radius must be that associated with the certification.

To achieve this, we performed comprehensive experimental validation against MNIST (LeCun et al., 1998) (GNU v3.0 license), CIFAR-10 (Krizhevsky et al., 2009) (MIT license), and the Large Scale Visual Recognition Challenge

variant of Imagenet (Deng et al., 2009; Russakovsky et al., 2015) (which uses a custom, non-commercial license). Each model was trained in PyTorch (Paszke et al., 2019) using a ResNet-18 architecture, with experiments considering two distinct levels of  $\sigma$ . Additional experiments involving the MACER (Zhai et al., 2020) certification framework and a ResNet-110 architecture can be found in Appendix D. The confidence intervals of expectations in all experiments was set according to the  $\alpha = 0.005$  significance level.

Our experiments involving our **Certification Aware Attack** set the offsets  $\delta_1$  and  $\delta_2$  to 1.05 and 0.95. That  $\delta_1 > 1$  ensures that the step is large enough to potentially induce a change in class, while setting  $\delta_2 \leq 1$  ensures that the predicted class does not change after an adversarial example has been identified. The resultant step sizes are then clipped to sit between 0.1 and 0.25 through Equation 14, to ensure that over-stepping doesn't occur. Details of the experiments that yielded these specific hyperparameter choices can be found in Appendix B.

Following previous experimental works, we employed the following hyperparameters for each attack framework. For **Carlini-Wagner**, we set the  $\kappa$  of Equation 3 to 0, and weighted the loss from the one-hot encoding by  $10^{-4}$ . The Carlini-Wagner training process was conducted using a learning rate of 0.01 over 100 iterations. Similarly **Deep-Fool** also employed 100 iterations, and employed an over-shoot factor of 0.02. The parameter space of **PGD** was informed by the parameter study of Appendix B, leading to  $\epsilon$  being set at  $\frac{20}{255}$  over 100 iterative steps. **AutoAttack** was performed using the randomised model variant, with the *maximum attack radii* set at  $\max\{5 \times R, 0.1\}$ , where  $R$  was calculated by Equation 6. AutoAttack was eschewed for Imagenet for runtime considerations.

Experiments on both MNIST and CIFAR-10 were performed upon a single NVIDIA A100 GPU core with 48 GB of GPU RAM (with maximum GPU RAM utilisation being on the order of 12 GB across all experiments), with expectations estimated over 1500 samples. Over the course of 50 epochs of training, each sample was perturbed with a single perturbation drawn from  $\mathcal{N}(0, \sigma^2)$  and added prior to normalisation. Training then utilised a batch size of 128, with losses assessed against the Cross Entropy loss. Parameter optimisation was performed with Adam (Kingma & Ba, 2014), with the learning rate set as 0.001. Imagenet was trained using a single A100 GPU, with 2 additional GPU's being employed for evaluation. Training occurred using SGD over 80 epochs, with a starting learning rate of 0.1, decreasing by a factor of 10 after 30 and 60 epochs, and momentum set to 0.9. As our current attack implementation does not incorporate any batching, to preserve system resources we decreased the number of samples associated with the expectation calculations in Imagenet to 600.

**Performance against other attacks** Across our full set of tested experiments, Figure 3 and Table 1 demonstrate that our new Certificate Aware Attack framework consistently constructs smaller adversarial perturbations than any other technique, with an average percentage reduction in the median radius of 8.5% relative to the next most performant approach in PGD. However, it must be emphasised that this is not strictly a like-for-like comparison, as each technique is capturing a different proportion of adversarial examples.

The magnitude of the performance increase relative to PGD appears to increase with the complexity of the input space, culminating with a 17.6% (at  $\sigma = 0.5$ ) and 34.5% (at  $\sigma = 1.0$ ) reduction in the median certified radius for Imagenet. This performance for Imagenet is revealing, in the context of the observation in Section 4.2 that all adversarial examples identified by our Certification Aware Attack framework must share the same class prediction as the first identified adversarial example for a given sample point. Intuitively such a drawback would appear to be substantially more limiting for the 1000 class Imagenet, as compared to MNIST or CIFAR-10, however it appears that this disadvantage is outweighed by the Certification Aware Attacks’ increased efficiency in exploring the potential search space.

The primary drivers of outperformance by our technique, relative to other comparable attacks, is our ability to iteratively refine the step size as we approach potential adversarial examples. For fixed step size attacks even if its iteration count was set to infinity, the fixed step size will ensure that the candidate solution oscillates about a local optima, rather than converging upon it. These efficiencies translate to an on average 87% reduction in the computational time across our experiments, relative to PGD.

Across the remainder of techniques, AutoAttack, Carlini-Wagner, and DeepFool all exhibit median perturbation radii that are multiples of what is observed from our technique, although it is notable that for Imagenet at  $\sigma = 1.0$  both Carlini-Wagner and DeepFool are able to identify significantly more adversarial examples than our approach, even if the associated perturbation radii was significantly higher. This is likely a product of suboptimal positioning in our  $(\delta_1, \delta_2, \epsilon_{\min}, \epsilon_{\max})$  parameter space in the high-dimensional, 1000-class Imagenet.

We also emphasise that the process espoused by our Certification Aware Attacks yields significant increases in the numerical efficiency of attacking these models, relative to the other attacks. In practice, Table 1 demonstrates that our approach can produce a more than 10-fold decrease in the computational time required to identify these attacks, relative to all approaches except DeepFool. However, that DeepFool’s perturbations are 3-times larger than our attacks underscores that the performance improvements yielded by our conceptual approach balance numerical efficiency

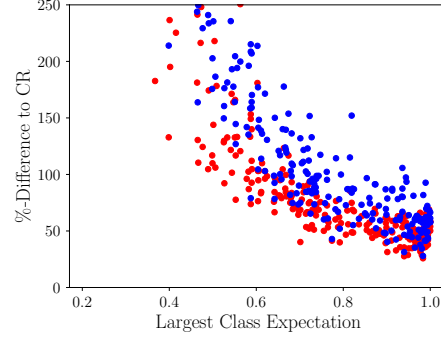


Figure 2. Percentage difference between constructed adversarial perturbations and the certified radii of Equation 6 for CIFAR-10 at  $\sigma = 0.5$ , with Our technique in red and PGD in blue.

against identifying norm-minimising perturbations.

**Performance relative to certified guarantees** While considering the differential performance of these adversarial attacks is valuable in and of itself, these experiments can also be used to explore how tight the certified guarantees provided by Equation 6 are. Such an analysis must also consider the influence of increasing  $\sigma$ , as it is well understood that increasing the level of noise to a certifiably robust model decreases the accuracy, while increasing the certification of the samples that it can certify. However, in the context of *attacking* these models, additional levels of noise inherently smooth the gradients, which should decrease the difficulty of attacking these models with gradient based methods. In practice Figure 3 demonstrates that the percentage difference between our new attack and the Cohen et al. certification radius of Equation 6 is relatively constant across the tested  $\sigma$  for all techniques. If it is true that increasing  $\sigma$  makes it easier to attack a model, this would suggest that this ease is being offset by the certification bounds tightening with  $\sigma$ .

To further illuminate the nature of the performance of our attack, Figure 2 considers the sample-wise performance of both PGD and our Certification Aware Attack. Within this data there is a clear self-similar trend, in which the percentage difference to Equation 6 increases as the largest class expectation decreases. This difference could indicate the potential for improving the certification of samples within this region. There also appears to be a correlation between the outperformance of our approach and the semantic complexity of the prediction task, which suggests that tightening these guarantees could be increasingly relevant for complex datasets of academic and industrial interest.

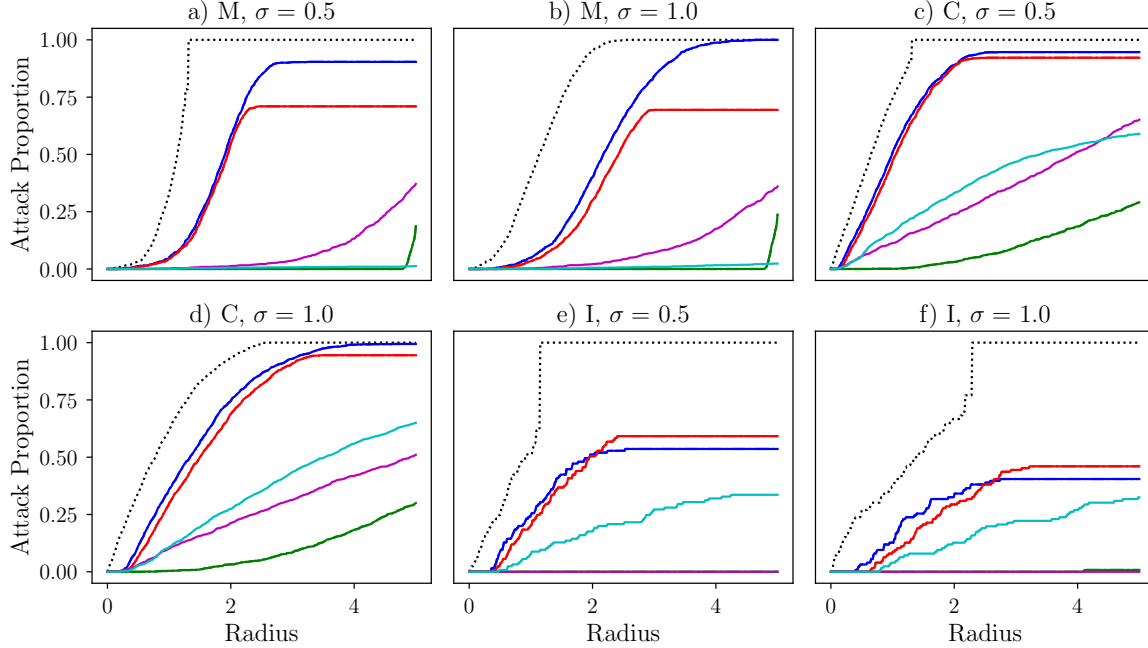


Figure 3. Best achieved Attack Proportion for our new Certification Aware Attack (blue), PGD (red), DeepFool (cyan), Carlini-Wagner (green), and AutoAttack (magenta). The black dotted line represents the theoretical best case performance following Equation 6.

## 6. Limitations

To this point, our work has considered  $L_2$ -norm measures of perturbation size, as such distances are aligned with the most common guarantees of certified robustness, which also exist within an  $L_2$ -space. While this inherently biases our approach towards datasets with image-structured data, the core concepts of attacking randomised smoothing, and of augmenting attack methodologies with the knowledge of regions of class invariance should be readily extensible to a broad array of data types and structures.

It must also be noted that an  $L_2$ -norm centred definition may not be appropriate in all contexts, and does not reflect the potential of rotational or translational modifications (Tian et al., 2018), nor functional attacks (Laidlaw & Feizi, 2019).

Finally, this attack requires access to significant amounts of GPU memory. Attacking a ResNet-18 model trained for CIFAR-10 required approximately 10 GB of GPU memory when smoothing was performed over 1500 samples, with significantly more memory required for attacking Imagenet-size datasets. This memory consumption is driven by our current implementation requiring all samples to be loaded into memory at once, prior to performing the gradient-based iterative step. While this process can be improved through batching, we chose not to follow this to focus upon the performance of the attack vector itself.

## 7. Conclusion

The addition of calibrated noise through randomised smoothing has a well documented history of improving adversarial robustness. Recently, randomised smoothing has been introduced as a simple yet effective means to certifying the robustness of arbitrary models with high probability. However, within this work we demonstrate that this very process of certification through randomised smoothing can also introduce a new attack surface, that allows models incorporating randomised smoothing to be *more easily attacked*.

Implementing this framework into Certification Aware Attacks allows us to leverage certifications of samples which both predict the benign and malicious classes to significantly decrease the size of the identified adversarial perturbations relative to state-of-the-art test-time attacks. Taking this approach would likely allow an attacker to influence more samples before being detected than any other attack, as it produces perturbations up to 34% smaller than the next best technique, while also requiring significantly less computational time to attack. Based upon these observations, it is clear that the benefits and risks of deploying certifiably robust models should be considered in the context of our newly discovered attack vector.



## References

- Athalye, A., Engstrom, L., Ilyas, A., and Kwok, K. Synthesizing robust adversarial examples. In *International Conference on Machine Learning*, pp. 284–293. PMLR, 2018.
- Biggio, B., Corona, I., Maiorca, D., Nelson, B., Šrndić, N., Laskov, P., Giacinto, G., and Roli, F. Evasion Attacks Against Machine Learning at Test Time. In *Joint European Conference on Machine Learning and Knowledge Discovery in Databases*, pp. 387–402. Springer, 2013.
- Carlini, N. and Wagner, D. Towards Evaluating the Robustness of Neural Networks. In *2017 IEEE Symposium on Security and Privacy (SP)*, pp. 39–57. IEEE, 2017.
- Chen, B., Xu, Y., and Shrivastava, A. Fast and Accurate Stochastic Gradient Estimation. *Advances in Neural Information Processing Systems*, 32, 2019.
- Chiang, P.-y., Ni, R., Abdelkader, A., Zhu, C., Studer, C., and Goldstein, T. Certified Defenses for Adversarial Patches. *arXiv preprint arXiv:2003.06693*, 2020.
- Cohen, J., Rosenfeld, E., and Kolter, Z. Certified Adversarial Robustness via Randomized Smoothing. In *International Conference on Machine Learning*, pp. 1310–1320. PMLR, 2019.
- Croce, F. and Hein, M. Reliable Evaluation of Adversarial Robustness with an Ensemble of Diverse Parameter-Free Attacks. In *International Conference on Machine Learning*, pp. 2206–2216. PMLR, 2020.
- Cullen, A. C., Montague, P., Liu, S., Erfani, S. M., and Rubinstein, B. I. Double bubble, toil and trouble: Enhancing certified robustness through transitivity. In *Advances in Neural Information Processing Systems*. NeurIPS, 2022.
- Deng, J., Dong, W., Socher, R., Li, L.-J., Li, K., and Fei-Fei, L. Imagenet: A large-scale hierarchical image database. In *2009 IEEE Conference on Computer Vision and Pattern Recognition*, pp. 248–255. Ieee, 2009.
- Dong, Y., Liao, F., Pang, T., Su, H., Zhu, J., Hu, X., and Li, J. Boosting Adversarial Attacks with Momentum. In *Proceedings of the IEEE Conference on Computer Vision and Pattern Recognition*, pp. 9185–9193, 2018.
- Dwork, C., McSherry, F., Nissim, K., and Smith, A. Calibrating Noise to Sensitivity in Private Data Analysis. In *Theory of Cryptography Conference*, pp. 265–284. Springer, 2006.
- Fu, M. C. Gradient Estimation. *Handbooks in operations research and management science*, 13:575–616, 2006.
- Gilmer, J., Adams, R. P., Goodfellow, I., Andersen, D., and Dahl, G. E. Motivating the Rules of the Game for Adversarial Example Research. *arXiv preprint arXiv:1807.06732*, 2018.
- Goodfellow, I. J., Shlens, J., and Szegedy, C. Explaining and Harnessing Adversarial Examples. *arXiv preprint arXiv:1412.6572*, 2014.
- Goodman, L. A. On Simultaneous Confidence Intervals for Multinomial Proportions. *Technometrics*, 7(2):247–254, 1965.
- Huang, L., Joseph, A. D., Nelson, B., Rubinstein, B. I. P., and Tygar, J. D. Adversarial machine learning. In *Proceedings of the 4th ACM Workshop on Security and Artificial Intelligence*, pp. 43–58, 2011.
- Jang, E., Gu, S., and Poole, B. Categorical Reparameterization with Gumbel-Softmax. *arXiv preprint arXiv:1611.01144*, 2016.
- Kingma, D. P. and Ba, J. Adam: A Method for Stochastic Optimization. *arXiv preprint arXiv:1412.6980*, 2014.
- Krizhevsky, A., Hinton, G., et al. Learning Multiple Layers of Features from Tiny Images. Technical report, University of Toronto, 2009.
- Laidlaw, C. and Feizi, S. Functional Adversarial Attacks. *arXiv preprint arXiv:1906.00001*, 2019.
- LeCun, Y., Bottou, L., Bengio, Y., and Haffner, P. Gradient-Based Learning Applied to Document Recognition. *Proceedings of the IEEE*, 86(11):2278–2324, 1998.
- Lecuyer, M., Atlidakis, V., Geambasu, R., Hsu, D., and Jana, S. Certified Robustness to Adversarial Examples with Differential Privacy. In *2019 IEEE Symposium on Security and Privacy (SP)*, pp. 656–672. IEEE, 2019.
- Levine, A. and Feizi, S. (de)Randomized Smoothing for Certifiable Defense against Patch Attacks. *Advances in Neural Information Processing Systems*, 33:6465–6475, 2020.
- Li, B., Chen, C., Wang, W., and Carin, L. Certified Adversarial Robustness with Additive Noise. In *Advances in Neural Information Processing Systems*, pp. 9459–9469, 2019.
- Lyu, Z., Guo, M., Wu, T., Xu, G., Zhang, K., and Lin, D. Towards Evaluating and Training Reliably Robust Neural Networks. In *Proceedings of the IEEE/CVF Conference on Computer Vision and Pattern Recognition*, pp. 4308–4317, 2021.

- Mirman, M., Gehr, T., and Vechev, M. Differentiable Abstract Interpretation for Provably Robust Neural Networks. In *International Conference on Machine Learning*, pp. 3578–3586. PMLR, 2018.
- Mohapatra, J., Weng, T.-W., Chen, P.-Y., Liu, S., and Daniel, L. Towards Verifying Robustness of Neural Networks against a family of Semantic Perturbations. In *Proceedings of the IEEE/CVF Conference on Computer Vision and Pattern Recognition*, pp. 244–252, 2020.
- Moosavi-Dezfooli, S.-M., Fawzi, A., and Frossard, P. DeepFool: A Simple and Accurate Method to Fool Deep Neural Networks. In *Proceedings of the IEEE Conference on Computer Vision and Pattern Recognition*, pp. 2574–2582, 2016.
- Papernot, N., McDaniel, P., Goodfellow, I., Jha, S., Celik, Z. B., and Swami, A. Practical Black-Box Attacks against Machine Learning. In *Proceedings of the 2017 ACM on Asia Conference on Computer and Communications Security*, pp. 506–519, 2017.
- Paszke, A., Gross, S., Massa, F., Lerer, A., Bradbury, J., Chanan, G., Killeen, T., Lin, Z., Gimelshein, N., Antiga, L., Desmaison, A., Kopf, A., Yang, E., DeVito, Z., Raison, M., Tejani, A., Chilamkurthy, S., Steiner, B., Fang, L., Bai, J., and Chintala, S. Pytorch: An Imperative Style, High-Performance Deep Learning Library. In Wallach, H., Larochelle, H., Beygelzimer, A., d’Alché Buc, F., Fox, E., and Garnett, R. (eds.), *Advances in Neural Information Processing Systems 32*, pp. 8024–8035. Curran Associates, Inc., 2019.
- Russakovsky, O., Deng, J., Su, H., Krause, J., Satheesh, S., Ma, S., Huang, Z., Karpathy, A., Khosla, A., Bernstein, M., et al. Imagenet large scale visual recognition challenge. *International Journal of Computer Vision*, 115(3): 211–252, 2015.
- Salman, H., Li, J., Razenshteyn, I., Zhang, P., Zhang, H., Bubeck, S., and Yang, G. Provably Robust Deep Learning via Adversarially Trained Smoothed Classifiers. In *Advances in Neural Information Processing Systems*, 2019a.
- Salman, H., Yang, G., Zhang, H., Hsieh, C.-J., and Zhang, P. A Convex Relaxation Barrier to Tight Robustness Verification of Neural Networks. In *Advances in Neural Information Processing Systems*, 2019b.
- Singh, G., Gehr, T., Püschel, M., and Vechev, M. An Abstract Domain for Certifying Neural Networks. *Proceedings of the ACM on Programming Languages*, 3(POPL): 1–30, 2019.
- Szegedy, C., Zaremba, W., Sutskever, I., Bruna, J., Erhan, D., Goodfellow, I., and Fergus, R. Intriguing Properties of Neural Networks. *arXiv preprint arXiv:1312.6199*, 2013.
- Tian, S., Yang, G., and Cai, Y. Detecting Adversarial Examples through Image Transformation. In *Thirty-Second AAAI Conference on Artificial Intelligence*, 2018.
- Wang, S., Zhang, H., Xu, K., Lin, X., Jana, S., Hsieh, C.-J., and Kolter, J. Z. Beta-CROWN: Efficient Bound Propagation with Per-Neuron Split Constraints for Neural Network Robustness Verification. *Advances in Neural Information Processing Systems*, 34, 2021.
- Weng, L., Zhang, H., Chen, H., Song, Z., Hsieh, C.-J., Daniel, L., Boning, D., and Dhillon, I. Towards Fast Computation of Certified Robustness for ReLU Networks. In *International Conference on Machine Learning*, pp. 5276–5285. PMLR, 2018.
- Xu, K., Shi, Z., Zhang, H., Wang, Y., Chang, K.-W., Huang, M., Kaillkhura, B., Lin, X., and Hsieh, C.-J. Automatic Perturbation Analysis for Scalable Certified Robustness and Beyond. *Advances in Neural Information Processing Systems*, 33, 2020.
- Zhai, R., Dan, C., He, D., Zhang, H., Gong, B., Ravikumar, P., Hsieh, C.-J., and Wang, L. MACER: Attack-free and scalable robust training via maximizing certified radius. In *International Conference on Learning Representations*, 2020.
- Zhang, H., Weng, T.-W., Chen, P.-Y., Hsieh, C.-J., and Daniel, L. Efficient Neural Network Robustness Certification with General Activation Functions. In Bengio, S., Wallach, H., Larochelle, H., Grauman, K., Cesa-Bianchi, N., and Garnett, R. (eds.), *Advances in Neural Information Processing Systems 31*, pp. 4939–4948. Curran Associates, Inc., 2018a.
- Zhang, H., Weng, T.-W., Chen, P.-Y., Hsieh, C.-J., and Daniel, L. Efficient Neural Network Robustness Certification with General Activation Functions. In *Neural Information Processing Systems (NeurIPS)*, 2018b.

---

**Algorithm 2** Class prediction and certification for the Certification Aware Attack algorithm of Algorithm 1.

---

```

1: Input: Perturbed data  $\mathbf{x}'$ , samples  $N$ , level of added noise  $\sigma$ 
2:  $\mathbf{y} = \mathbf{0}$ 
3: for  $i = 1:N$  do
4:    $y_j = y_j + 1$  if  $GS(f_\theta(\mathbf{x}' + \mathcal{N}(0, \sigma^2))) = j$  {Here  $GS$  is the Gumbel-Softmax}
5: end for
6:  $\mathbf{y} = \frac{1}{N}\mathbf{y}$ 
7:  $z_0, z_1 = \text{topk}(\mathbf{y}, k = 2)$  {topk is used as it is differentiable,  $z_0 > z_1$ }
8:  $\tilde{E}_0, \hat{E}_1 = \text{lowerbound}(\mathbf{y}, z_0), \text{upperbound}(\mathbf{y}, z_1)$  {Calculated by way of Goodman et al. (Goodman, 1965)}
9:  $r = \frac{\sigma}{2} (\Phi^{-1}(\tilde{E}_0) - \Phi^{-1}(\hat{E}_1))$ 
10: return  $\mathbf{y}, \tilde{E}_0, \hat{E}_1, R$ 

```

---

**Algorithm 3** Step size control for the Certification Aware Attack algorithm of Algorithm 1.

---

```

1: Input:  $\mathcal{S}_i$  is the set of  $(\mathbf{x}, r)$  pairings for previous certifications of samples predicting class  $i$  (sorted from oldest to newest), current candidate attack  $\mathbf{x}'$ , proposed attack direction  $\mathbf{d}$ , current certification radius  $r$ 
2:  $s = r$ 
3: Flag = True
4: while Flag == True do
5:   Flag = False
6:   for  $(\bar{\mathbf{x}}, r) \in \mathcal{S}_i$  do
7:     if  $\mathbf{x}' + s \times \mathbf{d} \in B_P(\bar{\mathbf{x}}, r)$  then
8:        $s = \arg \max_{s > 0} (\mathbf{x} + s \times \mathbf{d} \in B_P(\bar{\mathbf{x}}, r))$ 
9:       Flag = True
10:      Remove state  $(\bar{\mathbf{x}}, r)$  from  $\mathcal{S}_i$ 
11:     end if
12:   end for
13: end while
14: return  $s$ 

```

---

## A. Algorithms

To support the core algorithm outlined within Section 4.3, we now present two additional subroutines that handle both prediction and step size control. Algorithm 2 outlines the steps sampling process required to generate both the class prediction and the certification radius, which is expressed in terms of the lower and upper bounds of the largest and second largest class, respectively labelled as  $\tilde{E}_0$  and  $\hat{E}_1$ . These expectations are calculated by way of a Monte-Carlo approximation of  $\mathbf{y} = E[f_\theta(\mathbf{x}'; \sigma, N)]$ , subject to the application of a concentration inequality to quantify the underlying uncertainties.

Algorithm 3 describes how the effective step sizes can be calculated, to ensure that the next predicted class has the potential to differ from the last if an adversarial example has not yet been identified; or to preserve the predicted class if an adversarial example has already been found. Constructing the algorithm in this fashion implements both Sections 4.1 and 4.2.

## B. Parameter Exploration

To explore the influence of the step size control parameters of Equation 14, Figure 4 considers the influence of a range of these parameters upon key attack metrics. Of these, it's advantageous to minimise the computational time and the perturbation size while maximising the proportion certified. However, while the computational time can be minimised by setting  $\epsilon_{\min} = 0.1$ , there is a linear proportionality between  $\epsilon_{\min}$ , the perturbation size, and the proportion of samples certified. Within this work our choice of parameter space was chosen to prioritise minimising the perturbation size, in exchange for the small reduction in the number of samples that could be certified.

Similarly the parameter  $\epsilon$  from the PGD iterative Equation 2 is explored within Figure 5. Similar to our Certification Aware Attacks, these results reveal an inherent trade off between perturbation size, average time and proportion certified. As our primary focus has been comparing techniques in terms of their achieved perturbation size, we set  $\epsilon = \frac{20}{255}$  for all our

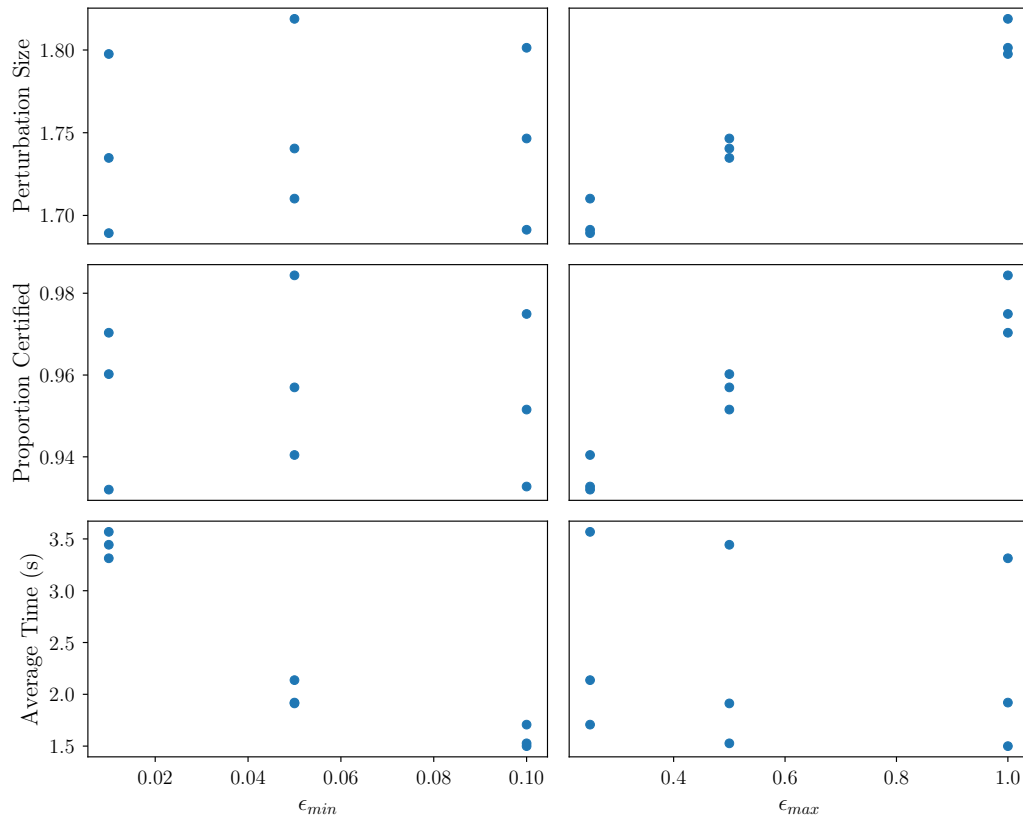


Figure 4. Parameter space for our Certification Aware Attacks in terms of the step size control parameters from Equation 14.



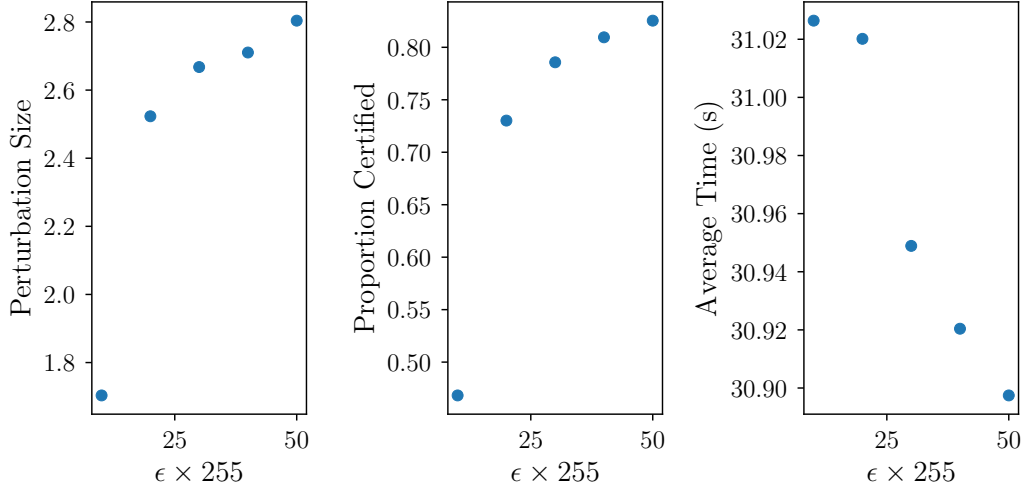


Figure 5. Parameter space for the PGD parameter  $\epsilon$  from Equation 2.

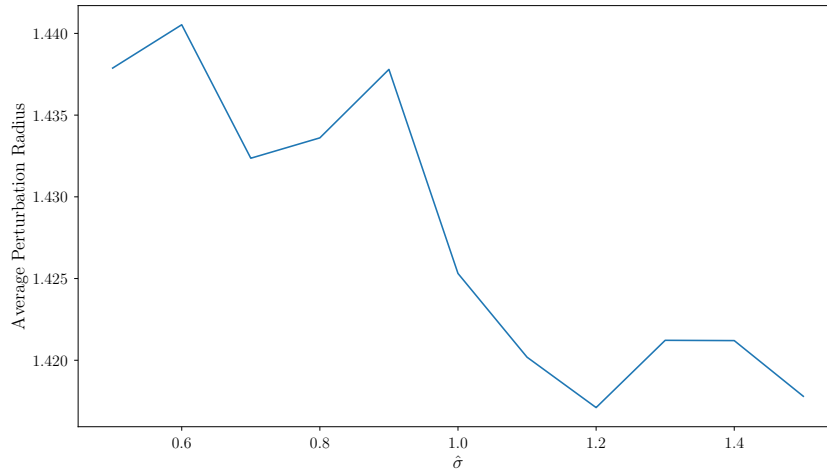


Figure 6. Average perturbation radius when  $\sigma$  is estimated by  $\hat{\sigma}$ . Data collected for CIFAR-10 at  $\sigma = 1.0$ .

experiments with PGD.

### C. Accuracy of $\sigma$

The white-box threat model assumes that the attacker has access to the full model and its parameters, including the level of additive noise  $\sigma$ . However, if the attacker only had access to the model and output class expectations, but was somehow shielded from accessing  $\sigma$  and  $r$ , it turns out that the Certification Aware Attack can still be applied subject to a sufficiently accurate guess of  $\sigma$ . As is shown by Figure 6, even over-estimating  $\sigma$  by 50% can decrease the radius of the identified adversarial perturbation under certain experimental conditions. That this is possible is a product of the terms  $\delta_1$  and  $\delta_2$  in Algorithm 1, as both of these parameters set the idealised step size to try and either change or preserve the predicted class. While this does suggest that there is potentially additional scope for optimising  $\delta_1$  and  $\delta_2$ , it also demonstrates that even estimating  $\sigma$  as part of a surrogate model, in order to attack under a limited white-box threat mode.

Table 2. Performance metrics for MNIST (M), CIFAR-10 (C), and Tiny-Imagenet (TI) for varying  $\sigma$  when trained using the MACER architecture. ‘Success’ and ‘Best’ are the proportion samples for which each attack was success, and outperformed all others.  $r_{50}$  and %-Cohen are the median attack and the size relative to the guarantee of Cohen et al..

Categorisation		Smallest Attack				
Data	Attack	Success	Best	$r_{50}$	%-Cohen	Time (s)
C-0.25	Ours	100%	72%	1.09	1276%	7.11
	PGD	55%	26%	0.90	1717%	26.21
	C-W	96%	0%	10.29	12307%	4.37
	D.Fool	100%	2%	2.28	2922%	9.53
C-0.5	Ours	94%	85%	1.68	1313%	11.32
	PGD	17%	8%	1.06	2300%	26.20
	C-W	88%	3%	10.68	7942%	4.70
	D.Fool	100%	5%	4.10	3467%	11.42
C-1.0	Ours	75%	72%	2.32	1330%	14.88
	PGD	4%	2%	1.31	2674%	26.17
	C-W	97%	13%	11.50	5547%	3.02
	D.Fool	100%	13%	7.37	4047%	9.53

## D. Training with MACER

Recent work has considered how the certified proportion of models can be improved by augmenting the training reward to maximising the expectation gap between classes (Salman et al., 2019a). A popular approach for this is MACER (Zhai et al., 2020), in which the training loss is augmented to incorporate what the authors dub as the  $\epsilon$ -robustness loss, which reflects proportion of training samples with robustness above a threshold level. In principle such a training time modification can increase the average certified radius by 10 – 20%, however doing so does increase the overall training cost by more than an order of magnitude.

To test the performance of our new attack framework against models trained with MACER, Table 2 and Figure 7 recreate earlier results from within this work for CIFAR-10, with a ResNet-110 architecture, rather than the ResNet-18 used in the remainder of this work. While the successful attack percentages, best attack proportions, and median certifications are roughly equal between both sets of experiments, there are significant differences in both the computational time—due to the larger model architecture—and the percentage difference between the certified radii and the attack size. This change in the percentage distance to the certification is a consequence of the Resnet-110 architecture (when trained under MACER) producing significantly smaller certifications than Resnet-18, with a median certification of 0.23 at  $\sigma = 1.0$ , relative to 1.32. That the attack radii are remaining constant while the certification radii decrease strongly suggests that there would be significant scope for improving the performance of these results with parameter space optimisation.

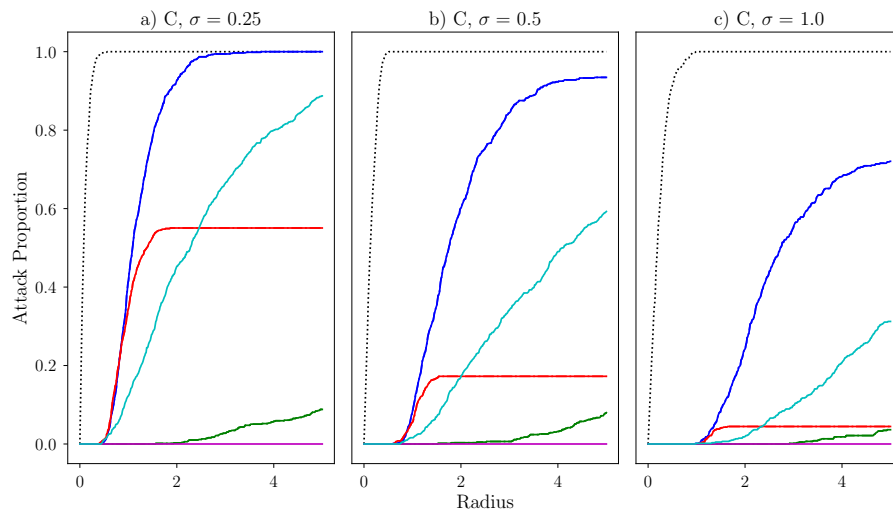


Figure 7. Attack and certification performance for a ResNet-110 model for CIFAR-10, when trained with MACER, covering our new Certification Aware Attack (blue), PGD (red), DeepFool (cyan), Carlini-Wagner (green), and AutoAttack (magenta). Similar to Figure 3, an ideal attack will approach the Cohen radii suggested by the black dotted lines.